CHEMMEDCHEM

DOI: 10.1002/cmdc.200800134

Stimulus Dependence of the Action of Small-Molecule Inhibitors in the CD3/CD28 Signalling Network

Karsten Köhler,[b] Alexander Ganser,[a] Thomas André,[b] Günter Roth,[b] Ludger Grosse-Hovest,[c] Gundram Jung,[c] and Roland Brock*[a, b]

Cells in the body are exposed simultaneously to a multitude of various signals. Inside a cell, molecular signalling networks integrate this information into a physiologically meaningful response. Interestingly, in the cellular testing of drug candidates, this complexity is largely ignored. Compounds are tested for cells that are challenged with one stimulus only. The activation of T lymphocytes through engagement of the T cell receptor (TCR)–CD3 complex and CD28 coreceptor is a prominent example for a cellular response that depends on the integration of signals. We investigated the cellular response characteristics of this network at different strengths of receptor and coreceptor activation. A novel cellular microarray-based approach, in which various combinations of antibodies directed against the CD3 complex and CD28 were spotted, was employed for analysing the stimulus dependence of activation of the transcription factor NFAT and actin reorganisation. For both responses, quantitative differences in inhibitor activity were observed. Remarkably, for IL-2 expression, which was detected by standard ELISA, low doses of the Src-family kinase inhibitor PP2 strongly potentiated IL-2 expression at high-level, but not at low-level, CD28 co-engagement. Therefore, for a physiologically highly relevant signalling network, the cellular response might vary qualitatively with only quantitative variations of a stimulus. This level of complexity should be considered in early cellular drug testing.

Introduction

The combination of sometimes conflicting signals into a physiologically meaningful response is a remarkable characteristic of the molecular signalling machinery. Signal transduction in T lymphocytes is paradigmatic for a sensitive dependence of a cellular response on the combination of stimuli from the molecular environment. Depending on the nature of the stimulus, the differentiation and activation state of a T cell and the molecular environment, a T cell can respond with activation and proliferation, anergy or apoptosis.[1] For the activation of naive T cells, two signals are necessary to induce persistent activation: the cross-linking of T cell receptor (TCR)/CD3 complexes by specific MHC/peptide complexes of antigen-presenting cells (APCs) and a co-stimulatory signal that is primarily provided through engagement of the CD28 coreceptor.[2] Given such different options for the cells to respond, one should therefore also expect variability in the biological activity of pharmacological agents. In fact, it has been shown already that CD28 co-stimulation might override the inhibitory activity of an immunosuppressant.[3] Nevertheless, to this point, analyses of the interplay of both stimuli in the CD3/CD28 signalling network were mostly conducted in a binary fashion. As a consequence, little detailed information exists on the interplay of both receptors in T cell activation. This deficit is also due to a shortfall in methods to efficiently probe the cellular response to large numbers of different stimuli.

We therefore sought to develop a strategy by which the interplay of signalling pathways in generating a cellular response could be analysed systematically, and to apply this strategy to testing the activity of low-molecular-weight inhibitors. Given its significance for the activation of cellular immunity, the CD3/CD28-dependent signalling network provides a highly interesting target for this approach. To sample systematically combinations of CD3 and CD28 stimuli, Jurkat T cell leukaemia cells were exposed to an antibody microarray in the presence or absence of pharmacological inhibitors. Each spot of the array contained a distinct mixture of stimulatory anti-CD3 and anti-CD28 antibodies, which provided a two-dimensional concentration matrix of both stimuli.

The arrays were produced in a microtitre plate format; this enabled an efficient processing of multiple samples. As a substitute for the APC, antibody-functionalised surfaces have been shown to reproduce major T cell signalling events.[4,5] Cell spreading as a measure for actin reorganisation and transloca-

[a] *A. Ganser, Prof. Dr. R. Brock*
Department of Biochemistry, Nijmegen Centre for Molecular Life Sciences
Radboud University Nijmegen Medical Centre
PO Box 9101, 6500 HB Nijmegen (The Netherlands)
Fax: (+31) 24-361413
E-mail: r.brock@ncmls.ru.nl

[b] *Dr. K. Köhler,[+] Dr. T. André,[++] Dr. G. Roth, Prof. Dr. R. Brock*
Department of Molecular Biology, Interfaculty Institute for Cell Biology
University of Tübingen, Auf der Morgenstelle 15, 72076 Tübingen (Germany)

[c] *Dr. L. Grosse-Hovest, Prof. Dr. G. Jung*
Department of Immunology, Interfaculty Institute for Cell Biology
University of Tübingen, Auf der Morgenstelle 15, 72076 Tübingen (Germany)

[+] *present address: Division of Cell and Molecular BiologyImperial College, South Kensington SW7 2AZ London (UK)*

[++] *present address: Bachem AG, Hauptstrasse 144, 4416 Bubendorf (Switzerland)*

Supporting information for this article is available on the WWW under http://dx.doi.org/10.1002/cmdc.200800134.

tion of the transcription factor NFAT were recorded by immunofluorescence microscopy followed by automated image analysis. In addition, by using a limited set of stimulus combinations, we probed for expression of the cytokine IL-2 by a standard ELISA assay.

All three T cell responses sensitively depended on the composition of the stimulus. For maximum activation, high-dose anti-CD28 stimulation was more essential than high-dose anti-CD3 stimulation. The effect of the inhibitors was stimulus- and dose-dependent. Remarkably, with respect to IL-2 expression at various combinations of anti-CD3 and anti-CD28, markedly different effects of low concentrations of the Src-family kinase-specific inhibitor PP2 were observed.[6] In the presence of high-dose anti-CD28, PP2 at concentrations $< 5\ \mu M$ strongly potentiated IL-2 expression. In the presence of high-dose anti-CD3 and low-dose anti-CD28, PP2 exclusively exerted an inhibitory effect. These results clearly demonstrate a stimulus-dependent activation of different signalling pathways. A mere testing of a combination of stimuli versus individual stimuli had failed to reveal this remarkable characteristic.

Results

When analysing the interplay of two stimuli at eliciting a cellular response, typically cells are exposed to a primary stimulus of different strength, and then the cellular response in the presence and absence of a second stimulus is recorded. While such analyses can reveal the general requirements for co-stimulation, they fail to resolve the mutual interdependence of two stimuli in eliciting a cellular response.

Here we set out to investigate the interplay of two stimuli in more detail, and how this interplay affects the activity of pharmacological inhibitors. We opted for the CD3 and CD28-dependent T cell response. Cellular antibody microarrays were developed as a new means to efficiently test many different combinations of stimuli with a minimum of cells. Cell spreading was quantified as a measure of actin reorganisation. Translocation of NFAT-1 was selected as an individual downstream signalling event. Both events are especially accessible to quantification by digital image processing.[7,8] Finally, IL-2 expression was assessed as a downstream event, because it integrates the inputs from several branches of the CD3 and CD28-dependent signalling network.

T cell attachment and activation on stimulatory antibody microarrays

Spreading of cells on antibody-coated glass surfaces provides a robust measure of activation-dependent actin reorganisation.[4] We had shown previously, that after fixation but not permeabilisation of cells, upon incubation of these surfaces with a fluorescently labelled antibody that was directed against the stimulating antibody, the part of the surface in contact with the cell was shielded from immunofluorescence staining.[7] The resulting dark patches provide a measure for cell spreading that is easily accessible to automated image processing.

To systematically probe the interplay of CD3 and CD28 in T cell activation, instead of coating surfaces with only one type of stimulus, a concentration matrix of stimulatory anti-CD3 and anti-CD28 antibodies was pipetted as a microarray by using a piezo-driven nanopipettor. In contrast to the testing of mere binary combinations of both stimuli, the concentration matrix eliminates arbitrariness with respect to the choice of concentrations of stimulatory agents, and provides detailed information on the cooperation of both signals. A polylysine spot served as a negative control to determine NFAT translocation in the absence of a stimulus. Furthermore, pipetting of multiple copies of these arrays in a microtitre plate format enabled the testing of the response of cells to the stimulatory antibody microarrays in the presence of different pharmacological inhibitors of individual signalling steps. After pipetting of the arrays, a frame was attached to the microarray substrate; this yielded 16 wells in a standard microtitre plate format per microarray substrate (Figure 1). In this way, in each well a multitude of different conditions, which corresponded to the number of spots of the microarray, could be tested. With one array per well, one order of magnitude more data is generated for a limited

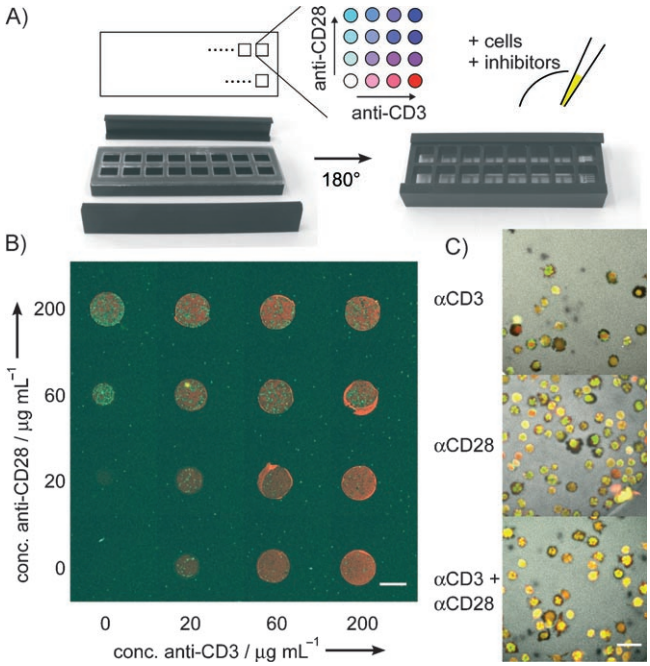

Figure 1. Anti-CD3/anti-CD28 antibody microarray. A) Experimental procedures for the processing of cellular antibody microarrays. Multiple copies of the antibody microarray are pipetted onto a hydrogel microarray substrate. Attachment of a frame creates 16 wells in the microtitre plate format. Cells and inhibitors are pipetted into the wells. Finally, the cells are fixed and stained for immunofluorescence microscopy. After removal of the frame, samples are mounted in anti-fading agent, sealed with a cover slip and imaged by confocal microscopy. B) Overview: mixtures of anti-CD3 and anti-CD28 antibodies were spotted at the indicated concentrations and visualised by staining with an Alexa546-labelled anti-mouse antibody (red). Jurkat cells are visualised by nuclear TOPRO staining (blue). As a control to mediate cell attachment without activation, polylysine was spotted. The scale bar represents 400 µm. C) Spreading and NFAT translocation of Jurkat cells on spots that are functionalised with 200 $\mu g\,mL^{-1}$ of anti-CD3, anti-CD28 or a mixture of both antibodies. The immobilised antibody is visualised in grey. Nuclei are coloured red, NFAT green, which results in a yellow colour in the case of co-localisation. The scale bar represents 20 µm.

number of cells—in our case, typically 100000 per well. In addition to determining the stimulus dependence of cell spreading, translocation of the transcription factor NFAT-1 was also quantified by using an immunofluorescence-based image processing protocol.

A succinimidyl ester-activated polyethylene glycol-based hydrogel was selected as a substrate for the generation of antibody microarrays. In comparison with epoxy-activated glass slides, for instance, the hydrogel-coated slides yielded a highly homogeneous distribution of antibodies within a spot over a wide concentration range (not shown). Moreover, cells attached only to antibody- or polylysine-functionalised parts of the substrate thereby enabling a direct correlation of attachment and spreading to activation.[9]

Cells were incubated on the microarrays for 60 min before fixation, which is the time required to observe pronounced NFAT translocation. In some cases, 20 $\mu g\,mL^{-1}$ of either antibody was not sufficient to induce the attachment of a sufficient number of cells to determine NFAT translocation. Overall, the number of cells per spot showed a positive correlation with antibody concentration in the range of ~5–200 cells with measurable properties present on each spot. Initial experiments had shown that spreading of Jurkat cells on anti-CD3 reached its maximum after ~10 min of cell stimulation, and was strongly reduced after 60 min, which is in accordance with reference [4], whereas on anti-CD28, spreading was stronger after 60 min than after 10 min (data not shown). These observations were confirmed and extended by the concentration matrix (Figure 2). Interestingly, after 60 min, cell spreading was reproducibly weaker on the spots that contained 200 $\mu g\,mL^{-1}$ anti-CD3 than on those that contained 60 $\mu g\,mL^{-1}$ anti-CD3 (Supporting Information figure S1). With regard to NFAT, anti-CD28 alone induced a stronger translocation than anti-CD3 alone. Again, cells that were exposed to a mixture of both antibodies showed an enhanced response, which was reproducibly strongest for the spots with maximum anti-CD28 concentration and intermediate anti-CD3 concentrations (Supporting Information figure S1). For both cell spreading and NFAT translocation, a gradient of activation was obtained for the whole array; this reveals that for the CD3/CD28 signalling network, different degrees of engagement of either receptor are sensitively translated into different responses.

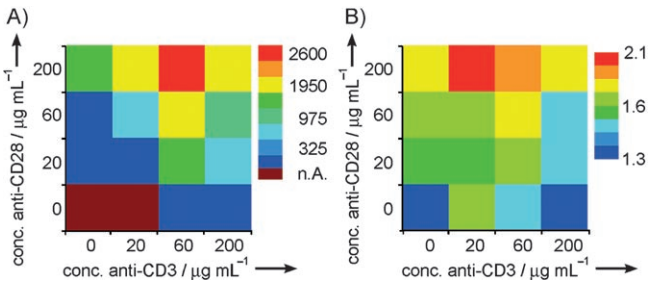

Figure 2. Cellular responses on an anti-CD3/anti-CD28 concentration matrix. A) Cell spreading is expressed as the average number of pixels covered per cell, with one pixel corresponding to 0.05 μm^2. B) Nuclear NFAT translocation expressed by the average of the ratios of fluorescence in the nucleus and fluorescence in the cytoplasm for each cell. An increased translocation is reflected by a higher ratio. The figures represent the averages of two (spreading) and three (translocation) experiments. Each coloured field corresponds to one spot in the microarray. The brown hue indicates that on this spot, cell spreading could not be quantified. The data for the polylysine spot (no antibody present/lower left corner) was included as a negative control.

It is evident that a cellular assay that operates with a maximum of a few hundred cells per sample (i.e., spot) has a considerable lower signal-to-noise ratio than, for example, reporter assays or ELISAs in which cellular responses are averaged over more than 10000 cells. Therefore, in our case, the availability of a criterion to assess the significance of results was a prerequisite for further analyses. We considered the fact that neighbouring spots exhibited gradual differences in the cellular response to be reliable criterion for the assessment of our results. The gradual dependence of the cellular response on the nature of the stimulus was confirmed by independent experiments that addressed the induction of IL-2 expression (see below). Moreover, the response profiles were well reproducible from day to day (Supporting Information figure S1).

The graded response matrix that was obtained for the activation of T cells demonstrates that for T cell activation, unlike, for instance, for epidermal-growth-factor-dependent signalling for which a switch-like response is observed,[10] the cellular response strongly depends on the strength of the stimuli.

Effects of small-molecule inhibitors

Having established that the anti-CD3/anti-CD28 antibody microarray yielded a gradient of the cellular responses over the whole concentration range, we next aimed to determine the effects of signalling inhibitors on this response profile. The specificity of these compounds is a general concern, and most compounds inhibit several targets.[11] However, our primary motivation was to assess whether potential differences in the activity of these drugs with respect to the CD3 and CD28-dependent activation of actin reorganisation and NFAT translocation existed. Only to a lesser extent were we interested in the role of the potential drug targets in these processes. The collection of inhibitors included established inhibitors of up- and downstream T cell signalling activities in the pathway that leads to NFAT activation (Figure 3). Cytochalasin D inhibits actin polymerisation and thus the formation of stable T cell contacts on anti-CD3-coated surfaces.[4,12] The Src family kinase inhibitor PP2 is a prototypical inhibitor of early CD3-dependent signalling with Lck as the primary target,[6] whereas piceatannol inhibits ZAP-70, a kinase directly downstream of Lck,[13] but has also been reported to inhibit PKC.[14] Alsterpaullone is an inhibitor of glycogen synthase kinase-3 (GSK-3),[15] however, it also inhibits Lck with a fivefold higher IC_{50} value.[16] GSK-3 antagonises the activity of the phosphatase calcineurin through NFAT phosphorylation. Calcineurin dephosphorylates NFAT, which leads to nuclear translocation.[17] SB-203580 has been described as a highly potent inhibitor of the MAP kinase p38.[18] With respect to NFAT, p38 has been shown to play a dual role. First, the kinase phosphorylates the transcription factor, thereby promoting nuclear export. Second, a p38-dependent induction of NFAT expression leads to an overall activation of NFAT-dependent transcription.[19] The concentrations applied for the indi-

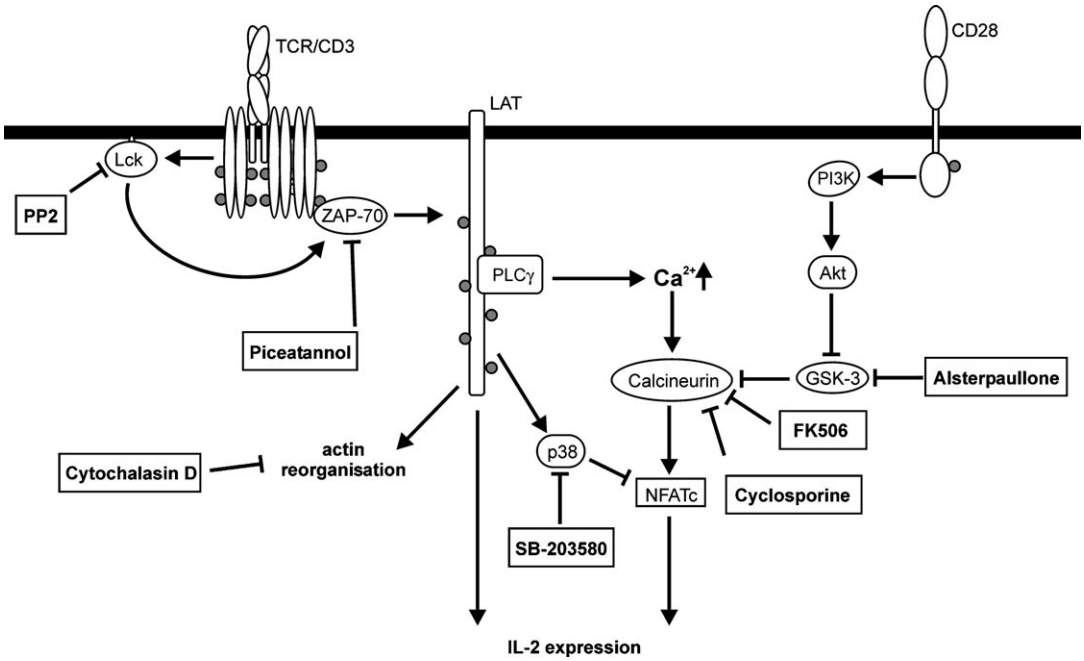

Figure 3. Schematic representation of the functional interdependence of the selected targets in the CD3/CD28 signalling network. TCR engagement leads to the recruitment of the Src-family kinase Lck, which phosphorylates tyrosine residues within the TCR/CD3 complex.[33] The Syk-family kinase ZAP-70 binds to the phosphorylated CD3ζ chains and propagates the activation by phosphorylating downstream components;[34] this leads to a phospholipase Cγ (PLCγ)-mediated increase in intracellular Ca^{2+} and the phosphorylation of membrane lipids by phosphatidylinositol-3′-kinase (PI3K). PLCγ-dependent calcium signalling leads to the activation of the phosphatase calcineurin, which dephosphorylates the nuclear factor of activation in T cells (NFAT), which leads to nuclear translocation.[17] The activity of calcineurin is antagonised by a glycogen synthase kinase-3 (GSK-3)-dependent phosphorylation of NFAT, which leads to the nuclear export of NFAT. GSK-3, in turn, is inhibited by a PI3K-dependent signalling pathway.

vidual inhibitors were selected based on concentrations that are commonly reported in the literature.

As expected for a compound that directly targets actin, 10 μM cytochalasin D exerted a uniform inhibitory effect on cell spreading. In addition, there was a slight decrease in NFAT translocation for those spots that contained high-dose anti-CD28 and a slight increase in translocation for those spots that contained only high anti-CD3 (Figure 4).

The Lck inhibitor PP2, on the other hand, uniformly inhibited NFAT translocation, and weakly inhibited cell spreading at the 60 min time point. Previously, a pronounced effect of PP2 on cell spreading had been reported.[4,7] In fact, spreading was much more strongly inhibited by PP2 when cells were fixed after 10 min (not shown). For piceatannol (10 μM), cell spreading was decreased for all combinations of stimulatory antibodies, whereas NFAT translocation was decreased most strongly for those spots that contained mixtures of anti-CD3 and anti-CD28 for which maximum NFAT translocation was observed. Both inhibitors of upstream kinase activities therefore showed clear differences in their response profiles that persisted at even higher concentrations of piceatannol (50 μM, not shown). For alsterpaullone, as expected for a GSK-3 inhibitor, a potentiation of NFAT translocation was observed. This effect was strongest for those spots that contained little anti-CD28, which is consistent with the fact that CD28-dependent activation of the kinase Akt, followed by phosphorylation and inactivation of GSK-3 is a rate-limiting step towards activation of NFAT. Cell spreading was not affected. For the p38 kinase inhibitor SB-203580 a slight inhibitory effect was present for spots with the highest anti-CD28 concentrations while for those spots with low anti-CD28 density, this inhibitor slightly activated translocation.

In summary, PP2 decreased NFAT translocation independent of the stimulus, whereas for cytochalasin D, piceatannol, SB-203580 and alsterpaullone, different inhibitory profiles were obtained for cells that were exposed to anti-CD3 or combinations of anti-CD3 and anti-CD28. The effects of these inhibitors, albeit in different ways, reduced the capacity of the network to distinguish different levels of CD3 and CD28 co-activation. Piceatannol exclusively exerted an inhibitory role, and significantly affected the potential of CD28 to enhance NFAT translocation. SB-203580 equalised the levels of NFAT translocation by exerting both activating and inhibitory roles and alsterpaullone strongly induced NFAT translocation for spots that contained little or no anti-CD28.

Stimulus and inhibitor dependence of IL-2 expression

After having shown that cell spreading and NFAT translocation responded sensitively to the composition of the CD3 and CD28-directed stimulus by using the cellular microarray-based approach, we next probed for the stimulus dependence of expression of the cytokine IL-2. IL-2 is a key inflammatory cytokine that is released by activated T cells. The IL-2 promoter integrates a large number of different signalling pathways.[20] Again, cells were stimulated with anti-CD3 alone, with anti-CD28 alone and with different mixtures of anti-CD3 and anti-CD28 (1:1, 1:0.25 and 0.25:1). For anti-CD3 alone, only a very

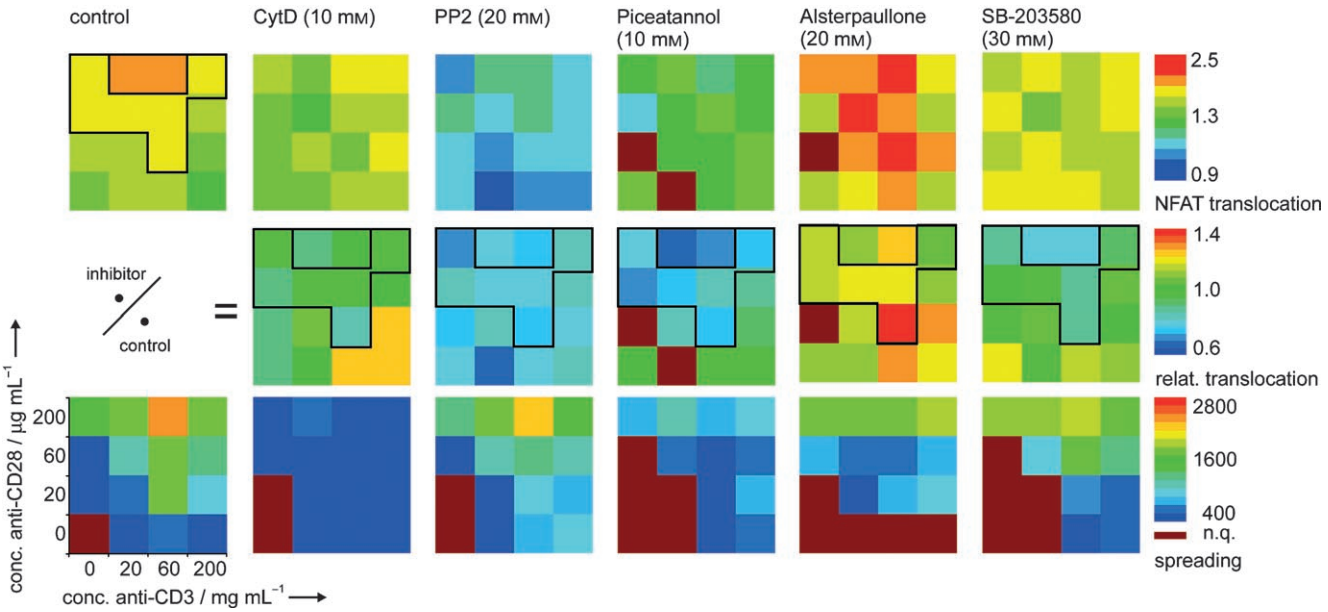

Figure 4. Response profiles in the presence of inhibitors. Top: NFAT translocation represented by the ratio of nuclear versus cytoplasmic fluorescence in the presence of inhibitor. Centre: relative effects of the inhibitors on NFAT translocation—ratio of nuclear versus cytoplasmic fluorescence in the presence of inhibitor was divided by the ratio in the absence of inhibitor. Blue hues represent an inhibitory effect, and yellow and red hues an activating effect on NFAT translocation. Bottom: cell spreading, expressed by the average number of pixels per cell. For spreading, absolute values instead of ratios of inhibited/noninhibited are shown. The data are averages of two to three experiments for each inhibitor. A brown square indicates those spots on the array for which in neither case a sufficient number of cells could be analysed. To assist the judgment of the stimulus dependence of the activity of the inhibitors, spots that induced comparable NFAT translocation for the control cells are outlined. The colouring scheme is different from the one in Figure 2 to enable a better assessment of activating and inhibitory effects.

weak IL-2 expression was induced. For cells that were stimulated with CD28 alone, no IL-2 expression was observed (not shown), therefore this stimulus was omitted from further experiments. Anti-CD3 and anti-CD28 in a 1:1 ratio elicited the strongest IL-2 expression, followed by anti-CD3/anti-CD28 0.25:1. Anti-CD3/anti-CD28 1:0.25 was less effective in inducing IL-2 expression; this is consistent with the microarray results for which high concentrations of CD28 were more potent in inducing NFAT translocation than high concentrations of anti-CD3 (Figure 5).

As inhibitors, we selected PP2 and alsterpaullone as well as the established immunosuppressants cyclosporine A and FK506. Both compounds inhibit activation of the phosphatase calcineurin. We were interested to learn whether alsterpaullone would decrease the observed differences between the individual stimuli by more effectively potentiating IL-2 expression by cells that were exposed to suboptimal stimuli, and whether PP2 would inhibit all responses to similar degrees.

In initial experiments we had observed that IL-2 expression reacted more sensitively to pharmacological inhibitors than NFAT translocation. Therefore, all inhibitors were titrated over individually adjusted concentration ranges. Cyclosporin A and

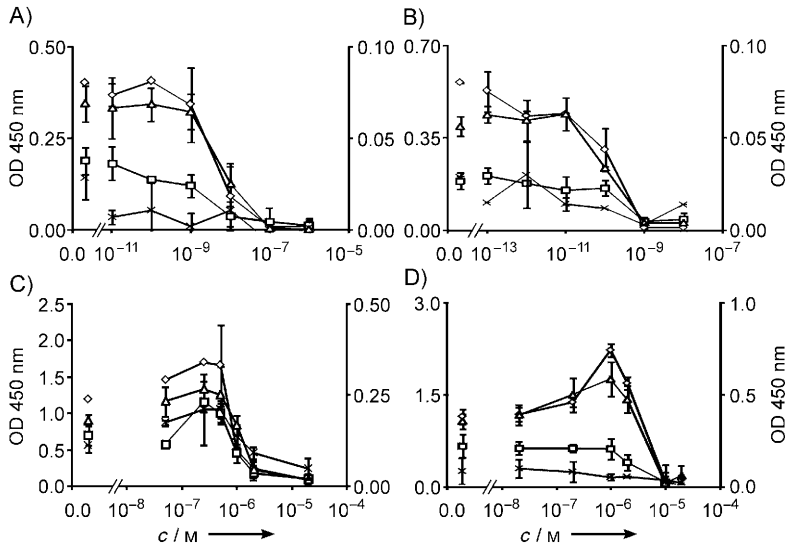

Figure 5. Stimulus dependence of IL-2 expression. Jurkat cells were stimulated with anti-CD3 and anti-CD28 at the indicated ratios in the absence and presence of different concentrations of A) cyclosporin, B) FK506, C) alsterpaullone, and D) PP2 and the induction of IL-2 expression was measured by matched-pair ELISA. The primary axis indicates IL-2 expression that was induced by anti-CD3/anti-CD28 in ratios of 0.25:1, 1:0.25 and 1:1, the secondary axis indicates IL-2 expression that was induced by anti-CD3 only. For each inhibitor, the results of three independent experiments are shown. Error bars are standard deviations of the mean. To account for day-to-day variations of OD values, for each inhibitor the OD values were normalised based on the OD value for the control, which was incubated with anti-CD3/anti-CD28 1:1 in the absence of inhibitor (diamonds: anti-CD3/anti-CD28 1:1, triangles: anti-CD3/anti-CD28 0.25:1, squares: anti-CD3/anti-CD28 1:0.25, crosses: anti-CD3 only).

FK506 uniformly inhibited IL-2 expression in a concentration-dependent manner (Figure 5A, B). Alsterpaullone at concentrations of up to ~0.5 μM potentiated IL-2 expression for all types of stimuli, thereby reducing the differences between CD3 stimulation alone and the other stimuli. However, at 10 μM, a concentration at which NFAT translocation was potentiated, IL-2 expression was strongly decreased for all types of stimuli. Very remarkably, the activity of PP2 varied in a stimulus-dependent way. Upon stimulation of cells with anti-CD3 alone and with anti-CD3/anti-CD28, 1:0.25, IL-2 secretion was inhibited in a concentration-dependent manner at PP2 concentrations >5 μM. In contrast, when cells were co-stimulated with a high dose of anti-CD28, incubation with PP2 at concentrations of up to 5 μM led to an increase of IL-2 expression in a concentration-dependent way, followed by a complete inhibition at the highest PP2 concentration of 20 μM. With respect to NFAT translocation, only quantitative differences with respect to the activity of inhibitors were observed for the various combinations of CD3/CD28-directed stimuli.

Discussion

To understand the activation of cells in a physiological context, it is required to understand how different signals are integrated into a cellular response. Here, we addressed in detail the interplay of CD3 and CD28 in T cell activation. Our analyses reveal that for Jurkat T cells, different degrees of CD3 and CD28 engagement are sensitively translated into different degrees of NFAT translocation, cell spreading and IL-2 expression.

For most small-molecule inhibitors, stimulus-dependent pharmacological profiles were obtained that varied with the degree of CD28 co-engagement. For NFAT translocation at low levels of CD28 co-engagement, the activities of alsterpaullone and SB-203580 most likely relate to the poor capacity of CD3 to induce Akt activation and thereby decrease NFAT phosphorylation. The kinetics of CD28-induced cell spreading were delayed relative to CD3-induced spreading (not shown); this demonstrates at least a different timing of downstream signalling, which leads to actin reorganisation.

For IL-2 expression, again, different compositions of the stimulus were translated into different degrees of activation. CD28 engagement alone failed to induce IL-2 expression. In this case, however, a combination of anti-CD3 and anti-CD28 stimuli in a 1:1 ratio led to the strongest response. This is different from NFAT translocation, which was more effectively induced by high anti-CD28/low anti-CD3 density. These findings, which were obtained by a quantitative variation of both stimuli, clearly illustrate the interplay of CD3 and CD28 in the CD3/CD28 signalling network: CD3 and CD28-dependent signalling activities contribute to different degrees to activation of the individual arms of the signalling network that are integrated on the IL-2 promoter. CD28 exerts its activity primarily by induction of NFAT translocation.

For IL-2 expression, very remarkably, the activity of PP2 strongly depended on the nature of the stimulus. At high-doses of anti-CD28, low doses of PP2 increased IL-2 expression. The PP2 concentrations at which this effect was observed were lower than those required to inhibit NFAT translocation. This PP2-induced increase in IL-2 expression is consistent with the observation that siRNA-mediated down-regulation of Lck-potentiated CD3-dependent downstream signalling.[21] This observation was considered to be in conflict with the fact that in Lck-defective Jurkat cells CD3-dependent IL-2 expression is completely inhibited. For these researchers it was impossible to decide whether their observations were due to the fact that the siRNA-dependent approach accomplished only partial down modulation of Lck or whether Lck-deficient cells had acquired further modifications that rendered them unresponsive. Our results, which were obtained by using pharmacological inhibitors suggest in fact a dose-dependent effect. However, in our case, a signal-enhancing effect of Lck inhibition was only observed upon stimulation of CD3 in combination with high-dose co-stimulation of CD28. This straightforward definition of the dose dependence of Lck inhibition illustrates the strength of a chemical-genetics-based approach in comparison with down-regulation of protein expression by using molecular-biology-based techniques.

We also tested PP2 at lower concentrations in the cellular microarray format. However, either no effect, or only a slight inhibitory effect were observed (not shown); this demonstrates that the PP2-sensitive inhibitory activity was not upstream of NFAT. In contrast to PP2, low concentrations of alsterpaullone potentiated both NFAT translocation and IL-2 expression in a stimulus-independent fashion. This finding is consistent with GSK-3 being the target of this inhibitor. Moreover, the result demonstrate that even though at higher concentrations alsterpaullone can also inhibit Lck, the effects that were observed here for the potentiation of IL-2 expression by PP2 and alsterpaullone are due to interference with different molecular targets. Otherwise, identical dose–activity profiles had to be expected for the cellular assays.

While the agreement of our results with the siRNA-induced down-regulation of Lck activity strongly indicates that the potentiation of IL-2 expression by PP2 might indeed be attributed to targeting of Lck, the presence of off-target effects as the basis of this observation should also be considered. PP2 also inhibits Csk (C-terminal Src kinase), albeit with an IC_{50} value that is about an order of magnitude higher than the one for Lck.[16] Csk inhibits Lck activity, therefore inhibition of Csk leads to a potentiation of Lck activity.[22,23] The use of PP2 as a tool to selectively address Lck activity next to Csk activity indicates that our observations might be fully attributed to the action of PP2 on Lck.[23] Nevertheless, it cannot be excluded that the balance of the activities of these two kinases or an unknown secondary target and therefore also the sensitivity to inhibition is a function of the nature of the stimulus.

The cellular antibody microarrays provided the means to systematically probe different combinations of stimuli in a microtitre plate format. With one array per well, an order of magnitude more data is generated for a limited number of cells—in our case typically 100 000 per well. Cellular microarrays were introduced into cellular immunity about four years ago.[24,25] In these first examples, the microarrays served the detection and characterisation of antigen-specific T cells. Our cellular antibody

microarray adds a further dimension to functional cellular analyses in T cell immunology. The simultaneous testing of many different stimuli in combination with two readouts, that is, cell spreading and NFAT translocation, provides abundant information on the interplay of stimuli in generating a cellular response. Multiplexing in a microtitre plate format and automated microscopy and image analysis of T cell signalling are key elements of our experimental strategy. The technology is readily compatible with further multidimensional readouts such as the testing for the translocation of other transcription factors or for the phosphorylation of a large number of signalling proteins, including high-resolution microscopy of the clustering of signalling proteins.[7,26–28] Cell spreading and protein clustering are prominent characteristics of T cell signalling. Therefore, microscopy-based analyses are required to address major aspects of this biological system.

In drug development, exposing cells to many different environments yields important information on the range of potential activities that a compound might elicit in the physiological context. As our results show, a mere binary combination of stimuli might be insufficient to reveal all of the possible activities. Especially for those biological systems that respond sensitively to slight variations in the composition of a stimulus, as shown here for CD3/CD28-dependent signalling in T cells, a quantitative variation of stimuli is required. The observations that were obtained here for the Src-family kinase inhibitor PP2 underscore the importance of testing drug candidates in the presence of a large variety of different combinations of stimuli and drug concentrations. The activity of this drug was a function of the nature of the stimulus, the drug concentration and finally the selected read-out. Whereas we have focused on analysing the interplay of CD3 and CD28, a large number of other coreceptors also modulate the cellular response upon T cell receptor stimulation; this adds several more dimensions of complexity to this system.[29]

The microarray-based approach will be limited to those coreceptors that can be stimulated by surface-bound ligands. However, for T cells a large number of coreceptors can be stimulated in this way.[29] Instead of testing 16 combinations for obtaining detailed dose–response profiles, the data on IL-2 expression demonstrates that four combinations might also be sufficient to grasp the stimulus dependence of drug action for this specific combination of stimuli. This will enable the incorporation of further stimulus combinations, also those that consist of a combination of three or more different stimuli. Further soluble modulators such as cytokines can be added to each well, together with a drug.

It is certainly unrealistic to assume that we will be able to fully mimic the in vivo complexity of drug action in an in vitro cellular assay. Prediction of the required complexity of such a combinatorial assay for a given drug candidate is a difficult task. Depending on the intended therapeutic effect there will be a preference for the testing of stimuli that potentiate activation, as in our case, or of those that promote inhibition.

A further layer of complexity is introduced by the presence of different cell populations, for instance in the case of T cells one must consider both effector T cells and regulatory T cells, which may be differently affected by a drug.[30] For dissecting the complexity of T cell signalling, our antibody microarrays are therefore an important first step for increasing the information content per assay. Given that kinase inhibitors play an increasing role as specific cancer therapeutics, the preclinical detection of potential immunomodulatory side effects should greatly benefit from a systematic testing of different combinations of stimuli.

Experimental Section

Reagents and cell lines: PP2 and piceatannol were obtained from Calbiochem (Schwalbach, Germany), Cytochalasin D, SB-203580, and alsterpaullone were purchased from Sigma (Taufkirchen, Germany), FK506 was purchased from LC Laboratories (Woburn, MA, USA). All inhibitors were added as indicated from freshly prepared aqueous solutions that were prepared from DMSO stock solutions. Cyclosporin A, which was dissolved in ethanol was a gift from Ingo Müller, University Children's Hospital (Tübingen, Germany). The stimulatory anti-CD3 (clone OKT3) and anti-CD28 antibodies (clone 9.3) were purified by protein A affinity chromatography (Pharmacia, Freiburg, Germany). Antibody solutions were dialysed against PBS and stored at 4 °C after filter-sterilisation (0.22 μm). The human T helper cell leukaemia cell line Jurkat was cultivated in RPMI (Pan Biotech, Aidenbach) with 10% FCS (Pan) at 37 °C/5% CO_2. Expression of surface antigens was validated by flow cytometry. Cell vitality after inhibitor incubation was controlled by using an MTT assay.

Microarray procedures: Antibody microarrays were generated by pipetting (6 nL/spot) solutions of antibodies in 300 mM sodium phosphate buffer, pH 8.5 with 0.005% Tween-20 (Fluka, Munich, Germany), 0.01% BSA and 0.5% trehalose (Sigma) on hydrogel microarray substrates (Slide H, Schott, Jena, Germany) by using a piezo-electric nanopipettor (NP2.0 GeSiM, Dresden, Germany) at dew point (16 °C). As a negative control 100 μg mL^{-1} poly-L-lysine (MW 150000–300000; Sigma) was used. Subsequently, arrays were stored for 16 h at 4 °C with 70% relative humidity. Afterwards, arrays were washed for 5 min with PBS with 0.5% Tween-20, then for 2×5 min with PBS. Reactive groups were quenched with 50 mM ethanolamine (Sigma) in 50 mM borate buffer, pH 8 for 1 h. After three washes with PBS, the surface was blocked with 0.1% BSA for 15 min.

Cellular antibody experiments: For parallel processing of several microarrays, a 16-well superstructure (ProPlate Multiarray System, Grace Biolabs, Eugene, OR, USA) was clamped onto the hydrogel slide. Cells that were suspended in serum-free RPMI medium (5×10^5 cells/mL) were preincubated with inhibitor for 15 min at 37 °C before being added into the well. After 60 min at 37 °C/5% CO_2, the medium was removed, the cells were fixed with 4% paraformaldehyde in PBS, first for 10 min at 4 °C, then for 15 min at room temperature, and washed with PBS (3×). To quantify the spreading of the cells on the surface, the surface that was not shielded by adherent cells was stained by incubation with an Alexa546-labelled anti-mouse antibody (4 μg mL^{-1} in PBS, 0.1% BSA, Molecular Probes, Eugene, OR, USA) 30 min at room temperature.[7] For visualisation of NFAT translocation, cells were then washed with PBS, permeabilised with saponin buffer (PBS, 0.1% saponin (Sigma), 0.1% BSA) and incubated with a FITC-labelled anti-NFAT-1 (i.e., NFATc2) IgG (1.25 μg mL^{-1}, BD Pharmingen, Heidelberg, Germany) in combination with the nuclear stain TOPRO (Molecular Probes, 100 nM) for 30 min in saponin buffer. After washing with saponin

buffer (3×), samples were fixed with 4% paraformaldehyde for 15 min, and washed with PBS (3×). Subsequently, the superstructure was removed, and the arrays were embedded in anti-fading reagent (10% Mowiol, Aventis, Frankfurt, Germany, in 100 mM Tris-HCl, pH 8.5, and 25% glycerol) and sealed with a cover slip.[31]

Image acquisition and data analysis: Fluorescence microscopy was performed on an inverted LSM 510 confocal laser scanning microscope by using a Plan-Neofluar 40×0.75 NA lens (Carl Zeiss, Göttingen, Germany). Image analysis was performed by using Metamorph (Universal Imaging, Downingtown, PA, USA). For each cell, nuclear translocation of NFAT and cell attachment were quantified by using a specially designed macro. Determination of NFAT translocation followed general protocols for the quantification of protein translocation.[8,32] We had opted for the implementation of our own image analysis routines to permit a correlation of NFAT translocation and cell spreading on the single-cell level. NFAT translocation was expressed as the ratio of fluorescence in the nucleus and in the cytoplasm. One should note that the intensity ratios do not quantitatively reflect the concentration of NFAT in both compartments. Because of the lobular shape of the cell nuclei in most cases, the nuclear mask also encompassed a contribution of cytoplasmic fluorescence. Cell spreading was evaluated by measuring the area of the surface that was shielded against staining with the secondary antibody, which was detectable as a dark patch.

Stimulus-dependent IL-2 expression: ELISA plates were coated with anti-CD3 and anti-CD28 antibodies (100 μL per well) in ratios of 1:1, 1:0.25, 0.25:1 diluted into PBS to a total immunoglobulin concentration of 2 $\mu g\,mL^{-1}$ or with 2 $\mu g\,mL^{-1}$ anti-CD3 alone for 3 h at 37 °C. After washing with RPMI 1640 medium that contained 10% inactivated FCS, the wells were blocked with PBS/4% BSA (200 μL; Sigma) for 1 h. Cells were diluted to a density of 1×10^6 cells/mL. The cell-suspension (120 μL) was incubated with RPMI1640/FCS (120 μL) that contained inhibitor at the indicated concentrations for 30 min in a flat-bottomed microtitre plate (Sarstedt, Nümbrecht, Germany) followed by transfer of this suspension (200 μL) into a well of the antibody-coated microtitre plate and incubation for 16 h at 37 °C. Each condition was carried out in triplicate.

IL-2 expression was determined by matched-pair ELISA (BD Pharmingen, Heidelberg, Germany) by using the cell supernatant (100 μL). A horseradish-peroxidase-based detection system (BD Pharmingen) was employed for detection. Absorption at 450 nm was measured by using an UV/Vis plate reader (SpectraMAX340, Molecular Devices, Ismaning, Germany).

Acknowledgements

We thank R. Bohnert for expert assistance in programming and image processing. K.K. was a scholar of the Graduiertenkolleg 794. R.B. gratefully acknowledges financial support from the Volkswagen Foundation ("Nachwuchsgruppen an Universitäten", I/77 472).

Keywords: cell activation · drug development · immunology · signal transduction · T lymphocytes

[1] J. I. Healy, C. C. Goodnow, *Annu. Rev. Immunol.* **1998**, *16*, 645–670.
[2] O. Acuto, F. Michel, *Nat. Rev. Immunol.* **2003**, *3*, 939–951.
[3] J. M. Slavik, D. G. Lim, S. J. Burakoff, D. A. Hafler, *J. Immunol.* **2001**, *166*, 3201–3209.
[4] S. C. Bunnell, V. Kapoor, R. P. Trible, W. Zhang, L. E. Samelson, *Immunity* **2001**, *14*, 315–329.
[5] L. I. Salazar-Fontana, V. Barr, L. E. Samelson, B. E. Bierer, *J. Immunol.* **2003**, *171*, 2225–2232.
[6] J. H. Hanke, J. P. Gardner, R. L. Dow, P. S. Changelian, W. H. Brissette, E. J. Weringer, B. A. Pollok, P. A. Connelly, *J. Biol. Chem.* **1996**, *271*, 695–701.
[7] K. Köhler, A. C. Lellouch, S. Vollmer, O. Stoevesandt, A. Hoff, L. Peters, H. Rogl, B. Malissen, R. Brock, *ChemBioChem* **2005**, *6*, 152–161.
[8] K. A. Giuliano, R. L. DeBiasio, R. T. Dunlay, A. Gough, J. M. Volosky, J. Zock, G. N. Pavlakis, D. L. Taylor, *J. Biomol. Screening* **1997**, *2*, 249–259.
[9] A. Hoff, T. André, R. Fischer, S. Voss, M. Hulko, U. Marquardt, K.-H. Wiesmüller, R. Brock, *Mol. Diversity* **2004**, *8*, 311–320.
[10] B. Schoeberl, C. Eichler-Jonsson, E. D. Gilles, G. Muller, *Nat. Biotechnol.* **2002**, *20*, 370–375.
[11] M. A. Fabian, W. H. Biggs, D. K. Treiber, C. E. Atteridge, M. D. Azimioara, M. G. Benedetti, T. A. Carter, P. Ciceri, P. T. Edeen, M. Floyd, J. M. Ford, M. Galvin, J. L. Gerlach, R. M. Grotzfeld, S. Herrgard, D. E. Insko, M. A. Insko, A. G. Lai, J. M. Lelias, S. A. Mehta, Z. V. Milanov, A. M. Velasco, L. M. Wodicka, H. K. Patel, P. P. Zarrinkar, D. J. Lockhart, *Nat. Biotechnol.* **2005**, *23*, 329–336.
[12] K. Katagiri, S. Matsuura, *J. Antibiot.* **1971**, *24*, 722–723.
[13] J. M. Oliver, D. L. Burg, B. S. Wilson, J. L. McLaughlin, R. L. Geahlen, *J. Biol. Chem.* **1994**, *269*, 29697–29703.
[14] B. H. Wang, Z. X. Lu, G. M. Polya, *Planta Med.* **1998**, *64*, 195–199.
[15] M. Leost, C. Schultz, A. Link, Y. Z. Wu, J. Biernat, E. M. Mandelkow, J. A. Bibb, G. L. Snyder, P. Greengard, D. W. Zaharevitz, R. Gussio, A. M. Senderowicz, E. A. Sausville, C. Kunick, L. Meijer, *Eur. J. Biochem.* **2000**, *267*, 5983–5994.
[16] J. Bain, H. McLauchlan, M. Elliott, P. Cohen, *Biochem. J.* **2003**, *371*, 199–204.
[17] F. Macian, *Nat. Rev. Immunol.* **2005**, *5*, 472–484.
[18] A. Cuenda, J. Rouse, Y. N. Doza, R. Meier, P. Cohen, T. F. Gallagher, P. R. Young, J. C. Lee, *FEBS Lett.* **1995**, *364*, 229–233.
[19] C. C. Wu, S. C. Hsu, H. M. Shih, M. Z. Lai, *Mol. Cell. Biol.* **2003**, *23*, 6442–6454.
[20] W. J. Freebern, C. M. Haggerty, I. Montano, M. C. McNutt, I. Collins, A. Graham, G. V. Chandramouli, D. H. Stewart, H. A. Biebuyck, D. D. Taub, K. Gardner, *Pharmacogenomics J.* **2005**, *5*, 305–323.
[21] T. Methi, J. Ngai, M. Mahic, M. Amarzguioui, T. Vang, K. Tasken, *J. Immunol.* **2005**, *175*, 7398–7406.
[22] L. M. Chow, M. Fournel, D. Davidson, A. Veillette, *Nature* **1993**, *365*, 156–160.
[23] Y. Liu, I. M. Sainz, Y. Wu, R. Pixley, R. G. Espinola, S. Hassan, M. M. Khan, R. W. Colman, *Exp. Cell Res.* **2008**, *314*, 774–788.
[24] Y. Soen, D. S. Chen, D. L. Kraft, M. M. Davis, P. O. Brown, *PLoS Biol.* **2003**, *1*, 429–438.
[25] J. D. Stone, W. E. Demkowicz, Jr., L. J. Stern, *Proc. Natl. Acad. Sci. USA* **2005**, *102*, 3744–3749.
[26] S. C. Bunnell, D. I. Hong, J. R. Kardon, T. Yamazaki, C. J. McGlade, V. A. Barr, L. E. Samelson, *J. Cell Biol.* **2002**, *158*, 1263–1275.
[27] Z. E. Perlman, M. D. Slack, Y. Feng, T. J. Mitchison, L. F. Wu, S. J. Altschuler, *Science* **2004**, *306*, 1194–1198.
[28] K. Sachs, O. Perez, D. Pe'er, D. A. Lauffenburger, G. P. Nolan, *Science* **2005**, *308*, 523–529.
[29] R. A. Kroczek, H. W. Mages, A. Hutloff, *Curr. Opin. Immunol.* **2004**, *16*, 321–327.
[30] R. Zeiser, D. B. Leveson-Gower, E. A. Zambricki, N. Kambham, A. Beilhack, J. Loh, J. Z. Hou, R. S. Negrin, *Blood* **2007**, *111*, 453–462.
[31] M. Osborn, K. Weber, *Methods Cell Biol.* **1982**, *24*, 97–132.
[32] P. Lang, K. Yeow, A. Nichols, A. Scheer, *Nat. Rev. Drug Discovery* **2006**, *5*, 343–356.
[33] E. K. Barber, J. D. Dasgupta, S. F. Schlossman, J. M. Trevillyan, C. E. Rudd, *Proc. Natl. Acad. Sci. USA* **1989**, *86*, 3277–3281.
[34] E. N. Neumeister, Y. Zhu, S. Richard, C. Terhorst, A. C. Chan, A. S. Shaw, *Mol. Cell. Biol.* **1995**, *15*, 3171–3178.

Received: April 30, 2008
Revised: May 15, 2008
Published online on July 4, 2008

